

Short Communication

Porous $\text{Co}_3\text{Mo}_3\text{N}$ Nanorods as an Effective Electrocatalyst for Li-O₂ Battery

Jian Lu¹, Jianling Li^{1*}, Zhixun Zhu¹, Yuguang Zhao¹, Cheng Chen¹, Feiyu Kang²

¹State Key Laboratory of Advanced Metallurgy, University of Science and Technology Beijing, No. 30 College Road, Haidian District, Beijing 100083, China

²Lab of Advanced Materials, Department of Materials Science and Engineering, Tsinghua University, Beijing 100084, China

*E-mail: lijianling@ustb.edu.cn

Received: 16 October 2015 / Accepted: 5 November 2015 / Published: 1 December 2015

Porous $\text{Co}_3\text{Mo}_3\text{N}$ nanorods were prepared by hydrothermal process combined with ammonia annealing and applied as catalyst in Li-O₂ battery cell. The battery with the porous $\text{Co}_3\text{Mo}_3\text{N}$ nanorods showed a higher initial discharge capacity of 7902.8 mAh/g_c at current density of 100 mAh/g_c than that with the pure Ketjen black. Moreover, the $\text{Co}_3\text{Mo}_3\text{N}$ -based electrode displayed lower overpotential and better cycling performance than that of the carbon-only cathode. Such performance can be associated with the synergistic effects of high electrocatalytic activity and porous structure of the $\text{Co}_3\text{Mo}_3\text{N}$ nanorods.

Keywords: Porous materials; Li-O₂; Electrocatalyst; $\text{Co}_3\text{Mo}_3\text{N}$

1. INTRODUCTION

Lithium-oxygen batteries with remarkably high theoretical energy density are considered as promising energy storage device of next generation[1]. For oxygen can be directly obtained from the environment, the theoretical energy density of Li-O₂ battery is about 11972Wh/kg, around 10 times higher than that of the current Li-ion battery[2-3]. However, lacking effective cathode catalysts is still a serious challenge for practical applications.

Effective electrocatalyst could accelerate the kinetic reactions so that improve the overall energy storage efficiency[4-5]. And it is well-known that nanostructured electrocatalysts can provided the more active sites due to their high surface area. Thus, effective catalysts at nanolevel are very advantageous in facilitating the ORR/OER for Li-O₂ batteries. Recently, transition nitrides, such as TiN-VN, VN, GN/TiN, MoN/N-C, MoN/NGN, $\text{Co}_3\text{Mo}_3\text{N}$ [6-11] have been studied for improving the

performance of Li-air battery. Among them, $\text{Co}_3\text{Mo}_3\text{N}$ is considered more promising[9]. However, to the best of our knowledge, the porous $\text{Co}_3\text{Mo}_3\text{N}$ nanorods hasn't been used in Li-air batteries, even rarely reported[12-21].

In this study, we first synthesized uniform morphology, porous nanorods of $\text{Co}_3\text{Mo}_3\text{N}$ and applied it in Li- O_2 batteries. Compared with bulk mesoporous product as reported[9], the product have ordered nanorod porous structure, resulting in a greater specific surface area and more catalytic active sites in electrode. Therefore, the porous electro-catalyst lowers the overvoltages, and improves the rate performance and cycle performance of batteries.

2. EXPERIMENTS

2.1. Synthesis of $\text{Co}_3\text{Mo}_3\text{N}$ nanorods

All the materials are analytical grade (Aladdin agent network). 0.1mmol $\text{CoCl}_2 \cdot 6\text{H}_2\text{O}$ and 0.1mmol $\text{Na}_2\text{MoO}_4 \cdot 2\text{H}_2\text{O}$ were respectively dissolved in 20 mL mixed solution (distilled water: absolute ethyl alcohol=2:1). Then $\text{Na}_2\text{MoO}_4 \cdot 2\text{H}_2\text{O}$ solution was added to $\text{CoCl}_2 \cdot 6\text{H}_2\text{O}$ solution dropwise under stirring. After stirring for 15 minutes, the mixture was then transferred into a 50ml stainless autoclave and kept in oven at 160°C for 15h. The resulting product was washed twice with purified water and dried at 120°C for overnight. Finally, purple $\text{CoMoO}_4 \cdot n\text{H}_2\text{O}$ was calcined at 500°C under argon for 2h to get CoMoO_4 . In a typical nitridation process. The CoMoO_4 was calcined at 750°C under ammonia for 2 h. Temperature control process was as follows, room temperature to 350°C , 5°C min^{-1} , 350 to 450°C , $0.5^\circ\text{C min}^{-1}$, 450 to 750°C , 2°C min^{-1} [20-22]. Then the nitride was cooled in flowing ammonia to room temperature and passivated using a gas mixture containing 1% O_2 .

2.2. Characterization

X-ray diffraction (XRD) pattern was characterized by X-ray powder diffractometer (XRD, Rigaku TTRIII) equipped with Cu K α radiation. The scanning rate was $8^\circ/\text{min}$. Scanning electron microscopy (SEM) analyses were performed by SEM(FESEM, Zeiss SUPRATM 55). The X-ray photoelectron spectroscopy (XPS) analysis was measured by AXIS ULTRA^{DL}D (Al K α , $h\nu=1486.6$ eV, Kratos). The EIS of batteries before and after charge were measured in VMP2 electrochemical workstation (Princeton Applied Research, USA). The work electrode was the porous electrode, the reference electrode and the counter electrode were lithium foil.

2.3. Li- O_2 cell preparation

The oxygen cathodes were fabricated by homogenously coating ink composed of a mixture of 30wt% $\text{Co}_3\text{Mo}_3\text{N}$ nanorods catalyst, 55wt% Ketjenblack EC600JD(KB), 15wt% PVDF or 85wt% KB, 15wt% polyvinylidene fluoride(PVDF) onto carbon paper. The mass loading of the slurry was about $1\text{mg}\cdot\text{cm}^{-2}$. Then the coin cells were assembled in a glove box filled with pure argon($\text{H}_2\text{O}\% <1\text{ppm}$,

$O_2 < 1\text{ppm}$), and tested in oxygen atmosphere. Galvanostatic discharge-charge test of the Li-O_2 battery was carried out on LAND CT2001A testers using 2032-type coin cells.

3. RESULTS AND DISCUSSION

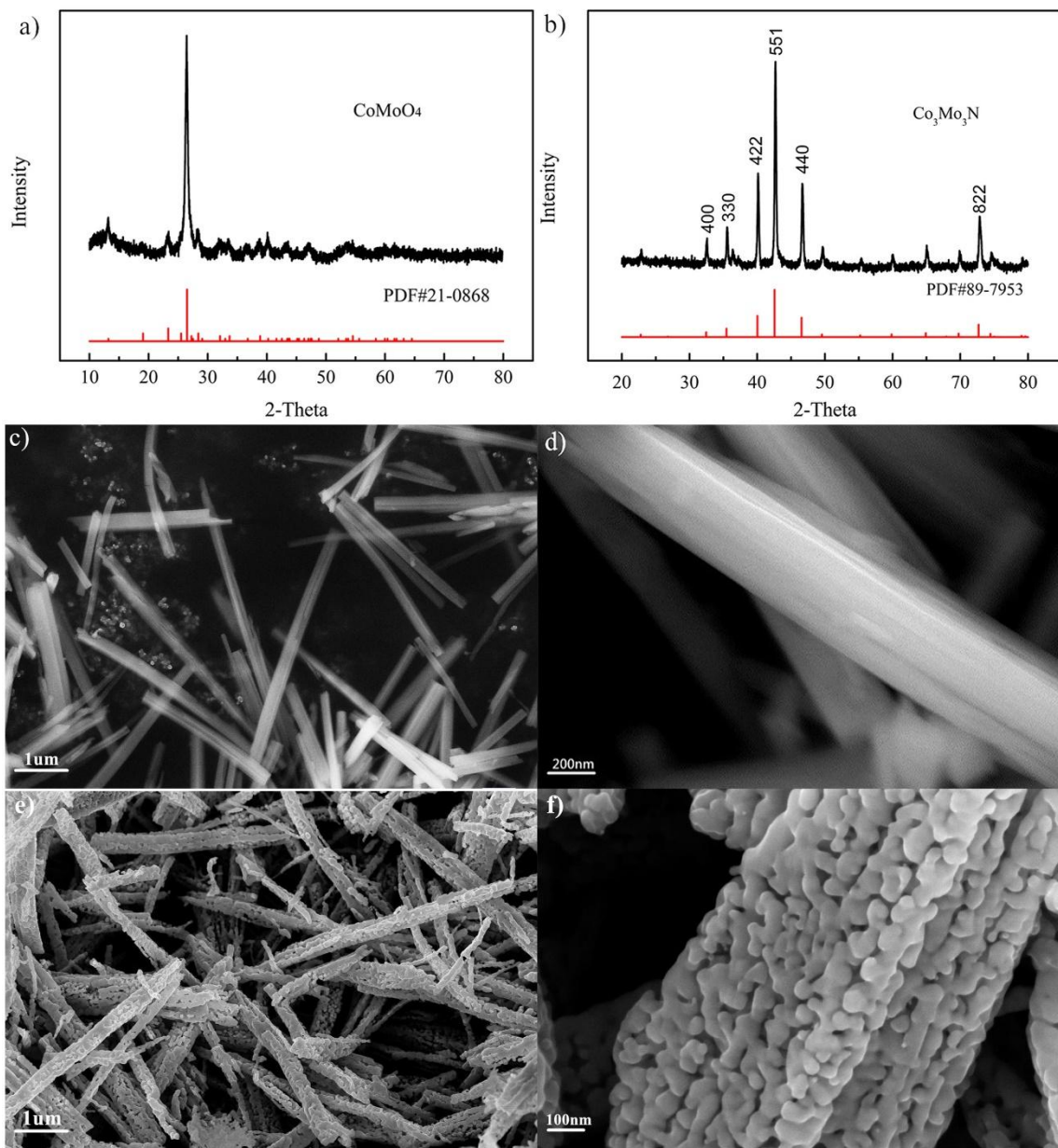


Figure 1. (a) XRD patterns of CoMoO_4 , (b) XRD patterns of $\text{Co}_3\text{Mo}_3\text{N}$, (c,d) SEM of CoMoO_4 , (e,f) SEM of $\text{Co}_3\text{Mo}_3\text{N}$

Fig.1(a) shows the XRD patterns of CoMoO_4 nanorods prepared by hydrothermal and calcination process. The peaks of XRD patterns can be indexed as the phase for CoMoO_4 (PDF#21-0868). Fig.1(b) illustrates the XRD patterns of the as-synthesized $\text{Co}_3\text{Mo}_3\text{N}$ nanorods recorded in the range of 2θ from 20° to 80° . The diffraction peaks are well-indexed to the (220), (400), (330), (422), (511), (440), and (822) planes of $\text{Co}_3\text{Mo}_3\text{N}$ phase (PDF#89-7953)[11,23]. And the sharp peaks

indicates the good crystallinity of the product. Fig.1(c), (d) and Fig.1(e),(f) respectively exhibit the SEM images of CoMoO_4 and $\text{Co}_3\text{Mo}_3\text{N}$. It is clear that in contrast to CoMoO_4 with smooth surface, there are many pores existing in $\text{Co}_3\text{Mo}_3\text{N}$ microstructure, which greatly increased the specific surface area of the product. So that more reaction interface can be provided.

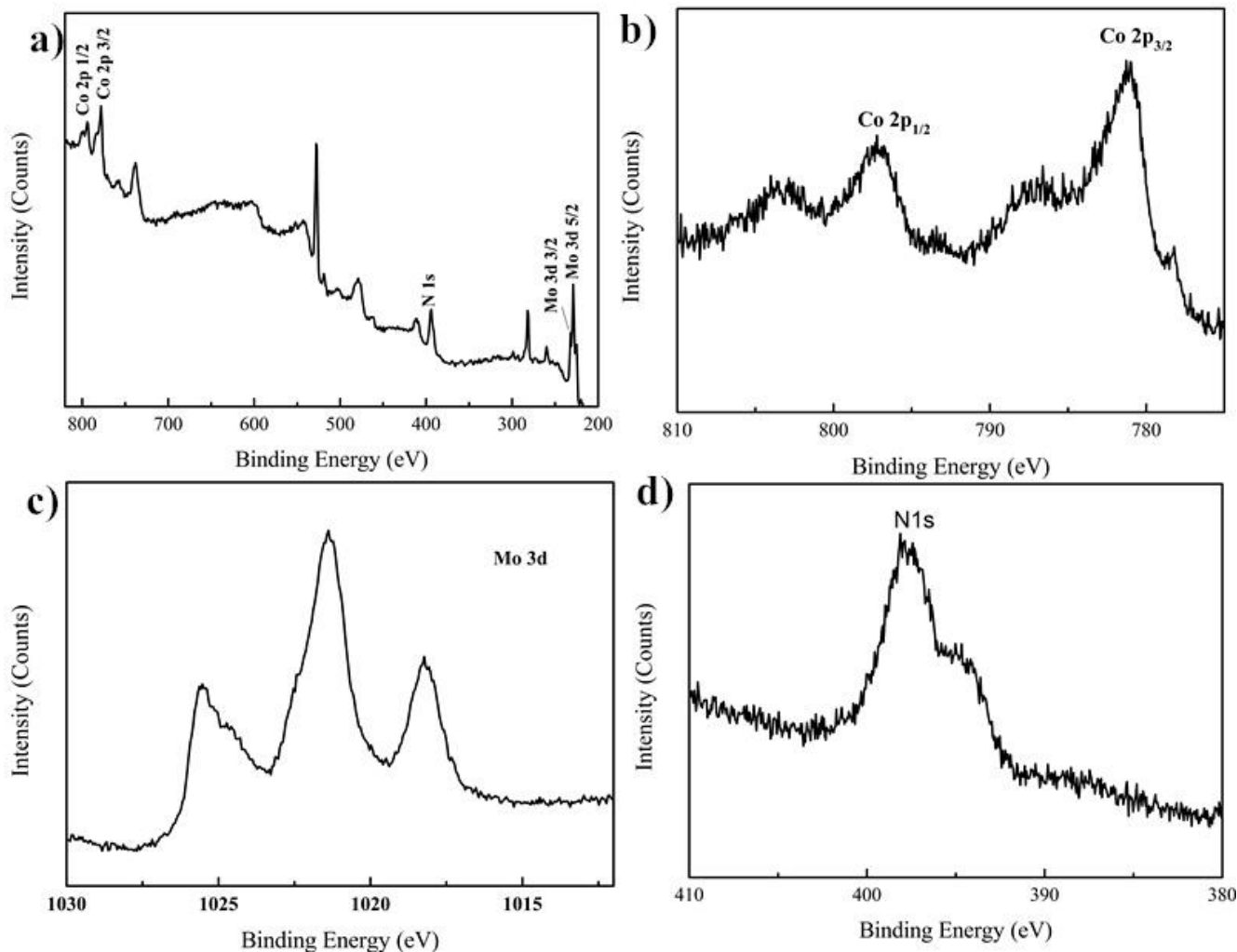


Figure 2. (a) XPS spectrum showing, (b) Co 2p XPS spectrum of $\text{Co}_3\text{Mo}_3\text{N}$, (c) Mo 3d XPS spectrum of $\text{Co}_3\text{Mo}_3\text{N}$, (d) N 1s XPS spectrum of $\text{Co}_3\text{Mo}_3\text{N}$.

The survey spectrum shown in Fig. 2(a) gives the elemental identity of the $\text{Co}_3\text{Mo}_3\text{N}$ sample. The high resolution spectra of Co 2p, Mo 3d and N 1s peaks are shown in Fig. 2(b), (c) and (d), confirming the presence of each element in the porous nanorods[11].

Fig. 3(a) shows the first voltage curves at a current density of 100mA/g_c , with a controlled discharging depth to 2.3V. The $\text{Co}_3\text{Mo}_3\text{N}$ -based cell outstanding exhibits first discharge capacity of 7902.8mAh/g_c , compared with carbon-based cells (6207.2mAh/g_c), as well as lower overpotential. At the current densities of 200, 500, and 1000mA/g_c , $\text{Co}_3\text{Mo}_3\text{N}$ electrode exerts specific capacities of 5217.2 , 3488.2 , and 1473.5mAh/g_c , which is higher than bare electrode. The long cycle stability was measured by limiting the discharge capacity to 500mAh/g_c at 100mA/g_c (Fig. 3b, Fig. 3c). The

$\text{Co}_3\text{Mo}_3\text{N}/\text{KB}$ electrode maintains 37 cycles with a stable discharging terrace (>2.3 V), while the KB electrode can just keep less than 10 cycles.

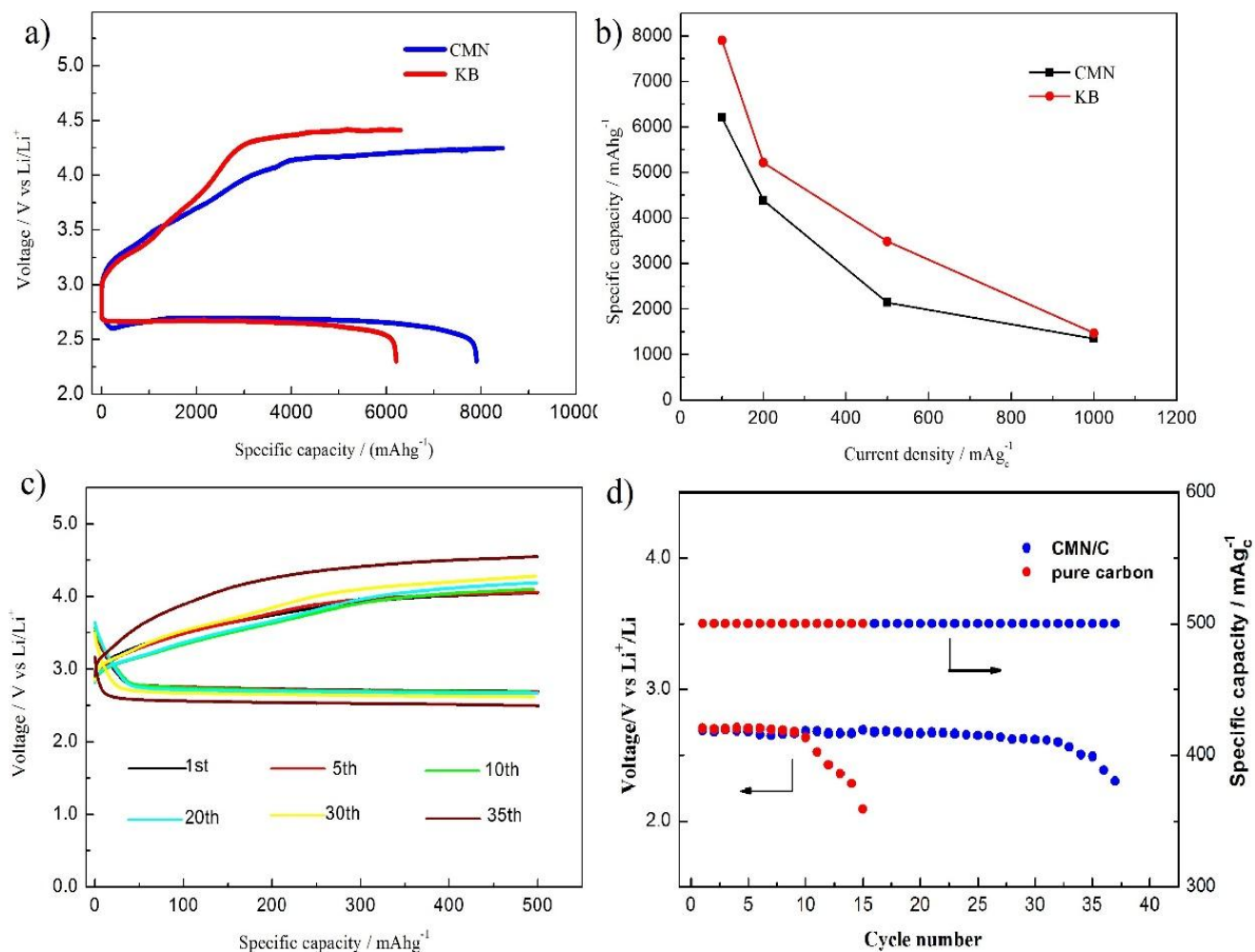


Figure 3. (a) First discharge-charge curves of $\text{Co}_3\text{Mo}_3\text{N}$ and bare electrodes at 100 mA/g_c , discharge specific capacity of $\text{Co}_3\text{Mo}_3\text{N}/\text{KB}$ and KB electrodes at different current densities. (b) Discharge specific capacity at different current densities. (c) Cyclic curves and (d) voltage of the terminal discharge of $\text{Co}_3\text{Mo}_3\text{N}$ and KB electrodes at 100 mA/g_c with limited capacity of 500 mAh/g_c

These results indicate that the porous $\text{Co}_3\text{Mo}_3\text{N}/\text{KB}$ electrode has better rechargeability and cyclability.

The electrodes were also studied using SEM. As shown in Fig. 4(a), the $\text{Co}_3\text{Mo}_3\text{N}$ electrode before discharging exhibited a rough surface. The nanoparticles were loosely dispersed in the carbon cloth. When discharged to 2000 mAh/g_c , flake-like, insoluble precipitate products formed on the surface. As the discharging progressed, the surface was completely covered with discharging products. Then after charging, the products disappeared and a relatively clean electrode was observed. The phenomenon showed that discharge product lithium peroxide could almost completely decomposed on $\text{Co}_3\text{Mo}_3\text{N}/\text{C}$ electrodes.

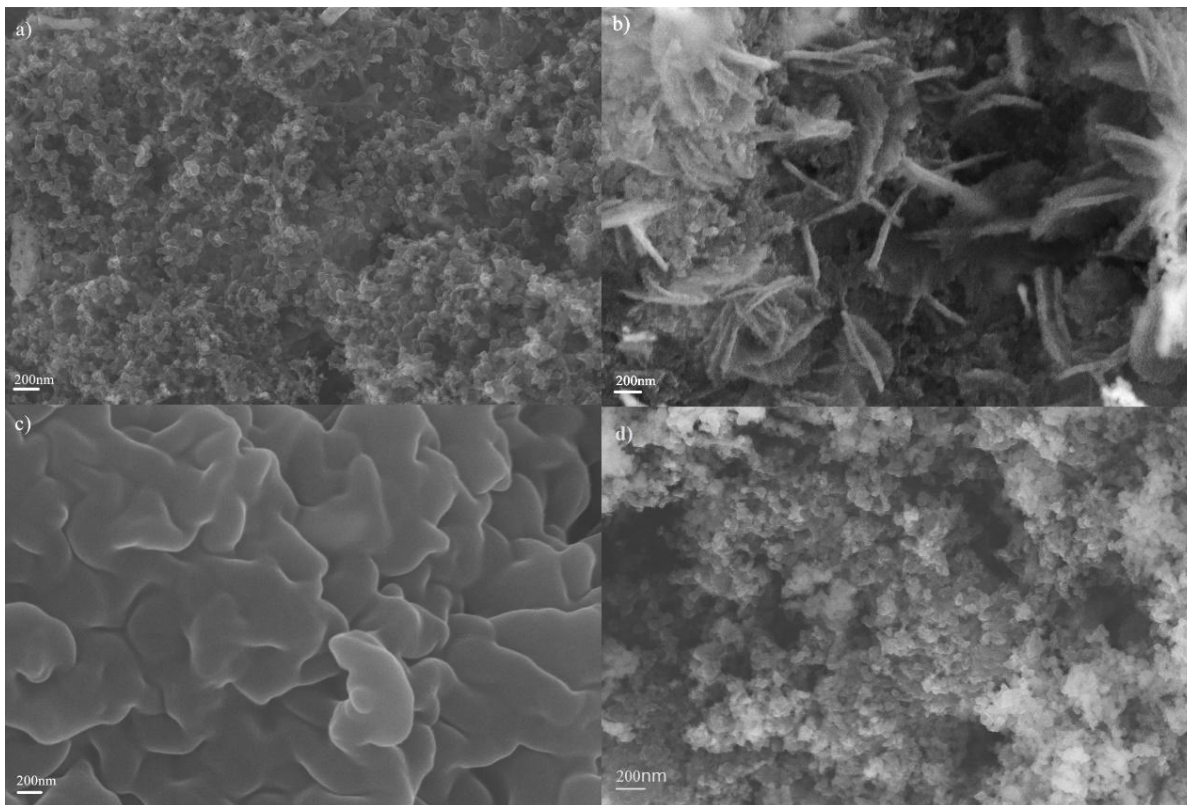


Figure 4. SEM images of the $\text{Co}_3\text{Mo}_3\text{N}/\text{KB}$ electrodes at different discharge-charge stages: (a) before discharge, (b) after discharging to 2000 mAh/g_c , (c) after full discharging, (d) after recharging.

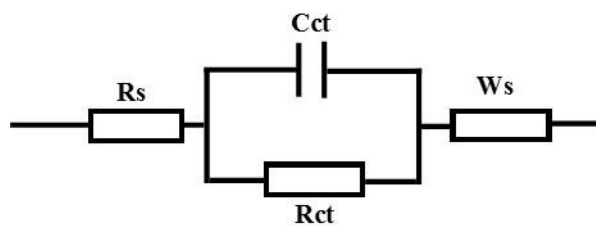


Figure 5. The equivalent resistance

In order to investigate the differences between catalyst electrode and bare electrode more clearly, electrochemical impedance spectroscopy (EIS) is performed in Fig.6. And the equivalent circuit is showed in Fig.5[24,25], where R_e represent the contact resistance between the electrode and current collector, the interfacial resistance between electrolyte and electrode. While R_{ct} is the charge transfer resistance, which is related to the kinetic reaction at the porous cathode. And we can generally determine the amount of discharge products by it in the reaction process. The values of R_{ct} fitted by EC-lab are listed in Table 1.

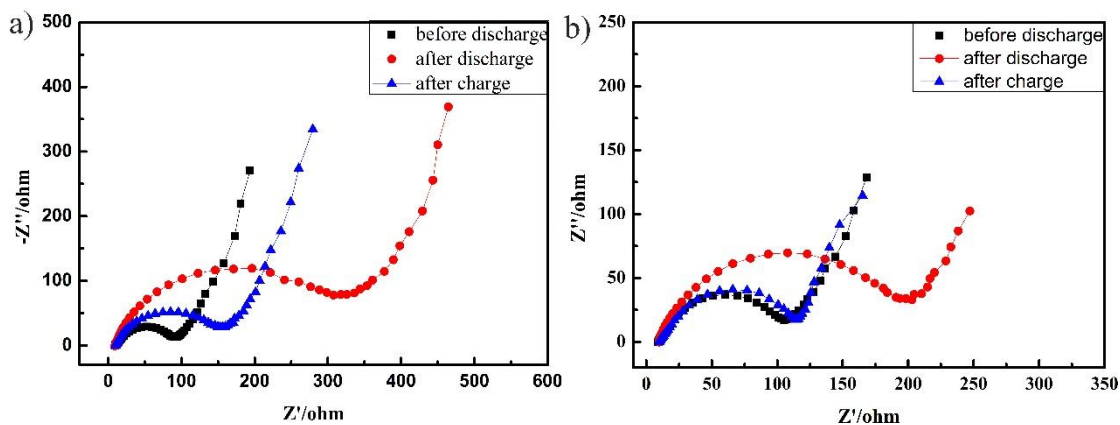


Figure 6. The EIS of Li-O₂ batteries (a) without or (b) with Co₃Mo₃N at different stages (100 mA/ g_c).

Table 1. Equivalent circuit parameters obtained from simulation of EIS experimental data.

current density (mA·g _c ⁻¹)	bare sample			CMN/KB sample		
	before discharge	after discharge	after charge	before discharge	after discharge	after charge
R _{ct} (Ω)	85.09	213.1	102	71.28	137.1	73.14

It is found that the value of R_{ct} of both Li-O₂ cells is very close before discharging. After the first discharge, the R_{ct} of both batteries increase significantly. The phenomenon is due to the formation of discharge product with poor electronic conductive. After the first charging process, the R_{ct} of bare sample is still high, for the existence of undecomposed discharge products. However, the Co₃Mo₃N electrode can almost recover the impedances, which is consistent with the SEM images of the electrode after charging (Fig. 4(d)).The phenomenon indicates that the catalytic effect of Co₃Mo₃N is excellent.

4. CONCLUSIONS

In summary, Porous Co₃Mo₃N nanorods was prepared via hydrothermal process combined with ammonia annealing, and employed as electrocatalyst for Li-O₂ batteries. Compared with the KB bare electrode, the Co₃Mo₃N/C sample exhibits lower overpotential, better rate performance and longer cycle life. The results indicate that the porous Co₃Mo₃N is an efficient electrocatalyst for non-aqueous Li-O₂ battery.

ACKNOWLEDGEMENTS

This work is supported by the National Natural Science Foundation of China (no.51172023), the National High Technology Research and Development Program of China (863 Program, 2012AA110302).

References

1. K. Zhang, H. Wang, X. He, Z. Liu, L. Wang, L. Gu, H. Xu, P. Han, S. Dong, C. Zhang, J. Yao, G. Cui, L. Chen, *Journal of Materials Chemistry*, 21 (2011) 11916.
2. K. Zhang, L. Zhang, X. Chen, X. He, X. Wang, S. Dong, L. Gu, Z. Liu, C. Huang, G. Cui, *ACS Applied Materials & Interfaces*, 5 (2013) 3677.
3. S. Dong, X. Chen, Chen, K. Chen, L. Gu, L. Zhang, X. Zhou, L. Li, Z. Liu, P. Han, H. Xu, J. Yao, C. Zhang, X. Zhang, C. Shang, G. Cui, L. Chen, *Chemical Communications*, 47 (2011) 11291.
4. J. Xu, Z. Wang, D. Xu, F. Meng, X. Zhang. *Energy & Environmental Science*, 7 (2014) 2213.
5. J. Wang, Y. Li, X. Sun, *Nano Energy*, 2 (2013) 443.
6. F. Cheng, J. Chen, *Chemical Society Reviews*, 41 (2012) 2172.
7. Y. Yue, P. Han, X. He, K. Zhang, Z. Liu, C. Zhang, S. Dong, L. Gu, G. Cui, *Journal of Materials Chemistry*, 22 (2012) 4938.
8. S. Korlann, B. Diaz, M. E. Bussell, *Chemistry of Materials*, 14 (2002) 4049.
9. K. Zhang, L. Zhang, X. Chen, X. He, X. Wang, S. Dong, P. Han, C. Zhang, S. Wang, L. Gu, G. Cui, *The Journal of Physical Chemistry C*, 117 (2013) 858.
10. J. Lee, S. Tai Kim, R. Cao, N. Choi, M. Liu, K. T. Lee, J. Cho, *Advanced Energy Materials*, 1(2011) 34.
11. P. G. Bruce, S. A. Freunberger, L. J. Hardwick, J. Tarascon, *Nature Materials*, 11 (2011) 19.
12. C. Chen, D. Zhao, D. Xu, X. Wang. *Materials Chemistry and Physics*, 95 (2006) 84.
13. C. Su, Y. Chang, S. Chang. *Materials*, 6 (2013) 5247.
14. I. A. Amar, R. Lan, C. T. G. Petit, S. Tao, *Electrocatalysis*, 6 (2015) 286.
15. X. Duan, G. Qian, X. Zhou, D. Chen, W. Yuan, *Chemical Engineering Journal*, 207-208 (2012) 103.
16. S. M. Hunter, D. H. Gregory, J. S. J. Hargreaves, M. Richard, D. Duprez, N. Bion, *ACS Catalysis*, 3 (2013) 1719.
17. S. Korlann, B. Diaz, M. E. Bussell, *Chemistry of Materials*, 14 (2002) 4049.
18. S. Podila, S. F. Zaman, H. Driss, Y. A. Alhamed, A. A. Al-Zahrani, L. Petrov, *A. Catal. Sci. Technol.*, 2015.
19. H. Wang, W. Li, M. Zhang, *Chemistry of Materials*, 17 (2005) 3262.
20. J. S. J. Hargreaves, D. Mckay, *Journal of Molecular Catalysis A: Chemical*, 305 (2009) 125.
21. D. Mckay, D. H. Gregory, J. S. J. Hargreaves, S. M. Hunter, X. Sun, *Chemical Communications*, 29 (2007) 3051.
22. H. Wang, W. Li, M. Zhang, *Chemistry of Materials*, 17 (2005) 3262.
23. S. Dong, X. Chen, L. Gu, X. Zhou, H. Wang, Z. Liu, P. Han, J. Yao, L. Wang, G. Cui, L. Chen, *Materials Research Bulletin*, 46 (2011) 835.
24. N. Sun, H. Liu, Z. Yu, Z. Zheng, C. Shao, *Solid State Ionics*, 268 (2014) 125.
25. H. Lv, R. Jiang, X. Zhang, J. Wang, Y. Li, *Int. J. Electrochem. Sci.*, 10 (2015) 7622.